Supporting Information

P4T-DOTA – A lanthanide chelating tag combining a sterically highly overcrowded backbone with a reductively stable linker

Daniel Joss[a] and Daniel Häussinger*[,a]

[a] Department of Chemistry, University of Basel, St. Johanns-Ring 19, CH-4056 Basel, daniel.haeussinger@unibas.ch

General Remarks

Unless otherwise stated, reactions were performed under an argon atmosphere and chemicals were used as received without further purification. Ubiquitin S57C and K48C were expressed as described previously by Sass et al., selectively ^{15}N leucine labelled hCA II S166C as described by Varghese et al.[1-2] Tagging reactions were performed with a conversion of > 95% at a protein concentration of 100 µM using 6.0 eq. (ubiquitin) or 10.0 eq. of the LCT (hCA II) in 10 mM phosphate and 0.3 mM TCEP buffer with pH 7.0 at rt overnight. ^{1}H-^{15}N HSQC and ^{1}H-^{15}N HSQC IPAP spectra were measured in 10 mM phosphate buffer with pH 6.0 (ubiquitin S57C and ubiquitin K48C) and pH 6.8 (hCA II S166C) at a temperature of 298 K on a 600 MHz Bruker Avance III NMR spectrometer equipped with a cryogenic QCI-F probe. The obtained NMR spectra were assigned using CcpNmr Analysis.[3] The tensor properties were then obtained by fitting the residues in secondary structure elements of ubiquitin (PDB 1UBI[4] and 2MJB[5]) or the leucine residues of hCA II (PDB 3KS3[6]) using Numbat.[7] The metal centres were found in a distance of 6.1-7.0 Å from the C_{beta} of the cysteine residue. PCS anisotropy parameters were derived exclusively from PCS data sets, while RDC anisotropy parameters were derived exclusively from RDC data sets with the metal position from the PCS data set as additional input. Q-factors were calculated using the following equation:

$$Q = \frac{\sqrt{\sum (PCS_{exp} - PCS_{calc})^2}}{\sqrt{\sum (PCS_{exp})^2}}.$$

^{1}H and ^{13}C NMR experiments were performed at a temperature of 298 K on a 600 MHz Bruker Avance III NMR spectrometer equipped with a cryogenic QCI-F probe. (2*S*,5*S*,8*S*,11*S*)-2,5,8,11-Tetraisopropyl-1,4,7,10-tetraazacyclododecane was synthesized according to the procedures described by Joss et al.[8], 5-(bromomethyl)-2-(methylthio)thiazolo[5,4-*b*]pyridine according to the procedures published by Müntener et al.[9] ESI-MS spectra were recorded on a Shimadzu LCMS-2020 liquid chromatograph mass spectrometer. HRMS spectra were measured on a Bruker MaXis 4G HiRes ESI Mass Spectrometer.

HPLC conditions

Analytical HPLC measurements were performed on a Shimadzu LC system (LC-20AT prominence liquid chromatograph, SIL-20A HT prominence auto sampler, CTO-20AC prominence column oven, CBM-20A communications bus module, SPD-20A prominence UV/VIS detector (λ = 254 and 280 nm, LC-20AD prominence liquid chromatograph) combined with a Shimadzu LCMS-2020 liquid chromatograph mass spectrometer. As column for analytical HPLC measurements, a ReproSil-Pur ODS, 3.3 µm, 150 x 3 mm, provided by Maisch GmbH was used. Commercial HPLC grade solvents were used and a binary gradient was applied.

Solvent A: Milli-Q water + 0.1% TFA

Solvent B: 90% acetonitrile + 10% Milli-Q water + 0.085% TFA.

HPLC gradient: 95% A (min 0-2), linear gradient 95% A to 100% B (min 2-6), 100% B (min 6-14), linear gradient 100% B to 95% A (min 14-15), 95% A (min 15-22).

Preparative HPLC purification was performed on a Shimadzu LC system (LC-20AT prominence liquid chromatograph, SIL-20A HT prominence auto sampler, CTO-20AC prominence column oven, CBM-20A communications bus module, SPD-20A prominence UV/VIS detector (λ = 254 and 280 nm, LC-20AD prominence liquid chromatograph) combined with a Shimadzu LCMS-2020 liquid chromatograph mass spectrometer. As column for preparative HPLC purification, a ReproSil-Pur 120 ODS-3, 5 µm, 150 x 20 mm, provided by Maisch GmbH was used. Commercial HPLC grade solvents were used and a binary gradient was applied during purification.

Solvent A: Milli-Q water + 0.1% TFA

Solvent B: 90% acetonitrile + 10% Milli-Q water + 0.085% TFA.

HPLC gradient: 95% A (min 0-2), linear gradient 95% A to 100% B (min 2-15), 100% B (min 15-22), linear gradient 100% B to 95% A (min 22-23), 95% A (min 23-25).

HPLC measurements of protein samples were performed using the direct injection mode on a Shimadzu LC system (LC-20AT prominence liquid chromatograph, SIL-20A HT prominence auto sampler, CTO-20AC prominence column oven, CBM-20A communications bus module, SPD-20A prominence UV/VIS detector (λ = 254 and 280 nm, LC-20AD prominence liquid chromatograph) combined with a Shimadzu LCMS-2020 liquid chromatograph mass spectrometer. Commercial HPLC grade solvents were used and a binary gradient was applied. MS spectra of proteins were deconvoluted using the Bruker Daltonics DataAnalysis software.

Solvent A: Milli-Q water + 0.1% TFA

Solvent B: 90% acetonitrile + 10% Milli-Q water + 0.085% TFA.

HPLC gradient: isocratic 95% A (min 0-4).

tri-*tert*-butyl 2,2',2''-((2*S*,5*S*,8*S*,11*S*)-2,5,8,11-tetraisopropyl-1,4,7,10-tetraazacyclododecane-1,4,7-triyl)(2*R*,2'*R*,2''*R*)-tripropionate

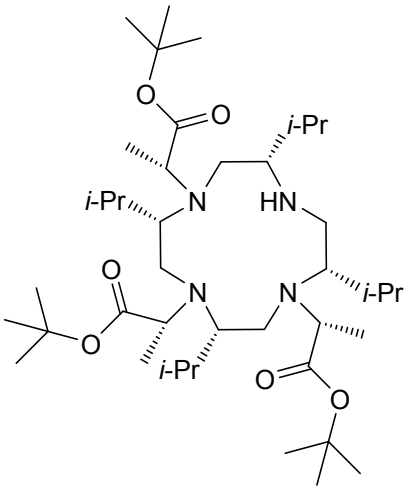

tert-Butyl (*S*)-2-(((trifluoromethyl)sulfonyl)oxy)propanoate (245 mg, 0.882 mmol, 3.0 eq.) in acetonitrile (0.5 ml) was added to (2*S*,5*S*,8*S*,11*S*)-2,5,8,11-tetraisopropyl-1,4,7,10-tetraazacyclododecane (100 mg, 0.294 mmol, 1.0 eq.) and potassium carbonate (406 mg, 2.94 mmol, 10.0 eq.) in acetonitrile (10 ml) and the mixture was stirred at rt overnight. The reaction was quenched by addition of an excess triethylamine, the solvent was evaporated under reduced pressure and the residue subjected to preparative HPLC to give tri-*tert*-butyl 2,2',2''-((2*S*,5*S*,8*S*,11*S*)-2,5,8,11-tetraisopropyl-1,4,7,10-tetraazacyclododecane-1,4,7-triyl)(2*R*,2'*R*,2''*R*)-tripropionate as white powder (133 mg, 62.4%).

HRMS: $[M+H]^+$, $C_{41}H_{81}N_4O_6$, m/z (calc.) = 725.6151, m/z (meas.) = 725.6158.

tri-*tert*-butyl 2,2',2''-((2*S*,5*S*,8*S*,11*S*)-2,5,8,11-tetraisopropyl-10-((2-(methylthio)thiazolo[5,4-*b*]pyridin-5-yl)methyl)-1,4,7,10-tetraazacyclododecane-1,4,7-triyl)(2*R*,2'*R*,2''*R*)-tripropionate

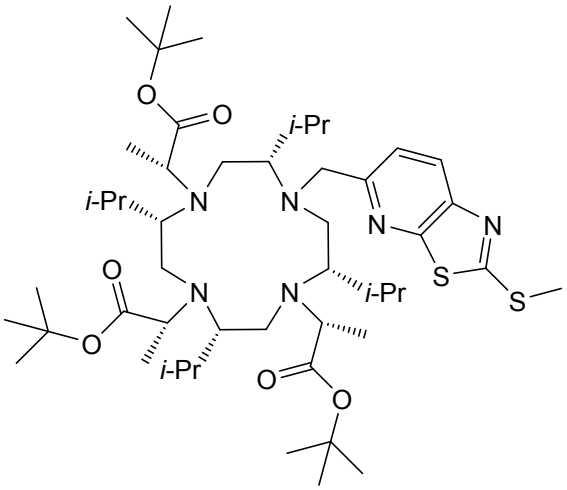

5-(bromomethyl)-2-(methylthio)thiazolo[5,4-*b*]pyridine (125 mg, 0.455 mmol, 2.6 eq.) was added to tri-*tert*-butyl 2,2',2''-((2*S*,5*S*,8*S*,11*S*)-2,5,8,11-tetraisopropyl-1,4,7,10-tetraazacyclododecane-1,4,7-triyl)(2*R*,2'*R*,2''*R*)-tripropionate (127 mg, 0.175, 1.0 eq.) in acetonitrile (10 ml) and the mixture was stirred for 4 h. Then potassium iodide (75.5 mg, 0.455 mmol, 2.6 eq.) was added and the mixture was stirred for 3 d at rt. The mixture was filtered and the solvent evaporated under reduced pressure. The residue was subjected to preparative HPLC to give tri-*tert*-butyl 2,2',2''-((2*S*,5*S*,8*S*,11*S*)-2,5,8,11-tetraisopropyl-10-((2-(methylthio)thiazolo[5,4-*b*]pyridin-5-yl)methyl)-1,4,7,10-tetraazacyclododecane-1,4,7-triyl)(2*R*,2'*R*,2''*R*)-tripropionate as white powder (75 mg, 46.6%).

HRMS: $[M+H]^+$, $C_{49}H_{87}N_6O_6S_2$, m/z (calc.) = 919.6123, m/z (meas.) = 919.6115.

(2*R*,2'*R*,2''*R*)-2,2',2''-((2*S*,5*S*,8*S*,11*S*)-2,5,8,11-tetraisopropyl-10-((2-(methylthio)thiazolo[5,4-*b*]pyridin-5-yl)methyl)-1,4,7,10-tetraazacyclododecane-1,4,7-triyl)tripropionic acid

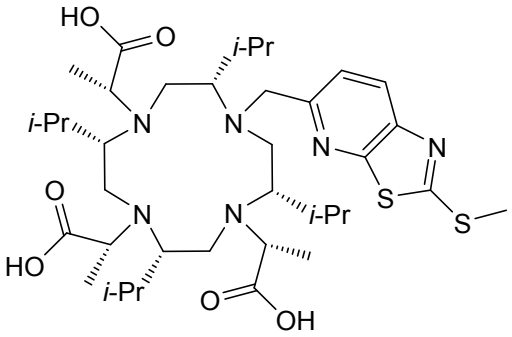

tri-*tert*-butyl 2,2',2''-((2*S*,5*S*,8*S*,11*S*)-2,5,8,11-tetraisopropyl-10-((2-(methylthio)thiazolo[5,4-*b*]pyridin-5-yl)methyl)-1,4,7,10-tetraazacyclododecane-1,4,7-triyl)(2*R*,2'*R*,2''*R*)-tripropionate (64.0 mg, 0.070 mmol, 1.0 eq.) was dissolved in a mixture of TFA, thioanisole and water (92:6:2, 5 ml) and stirred for 5 h at rt. Then the mixture was heated to 50 °C for 30 min and solvents were evaporated under reduced pressure. The residue was subjected to preparative HPLC to give (2*R*,2'*R*,2''*R*)-2,2',2''-((2*S*,5*S*,8*S*,11*S*)-2,5,8,11-tetraisopropyl-10-((2-(methylthio)thiazolo[5,4-*b*]pyridin-5-yl)methyl)-1,4,7,10-tetraazacyclo dodecane-1,4,7-triyl)tripropionic acid as a colourless glassy solid (40 mg, 76.3%).

HRMS: $[M+H]^+$, $C_{37}H_{63}N_6O_6S_2$, m/z (calc.) = 751.4245, m/z (meas.) = 751.4246.

Ln-(2*R*,2'*R*,2''*R*)-2,2',2''-((2*S*,5*S*,8*S*,11*S*)-2,5,8,11-tetraisopropyl-10-((2-(methylthio)thiazolo[5,4-*b*]pyridin-5-yl)methyl)-1,4,7,10-tetraazacyclododecane-1,4,7-triyl)tripropionate, Ln-P4T-DOTA$_{red}$

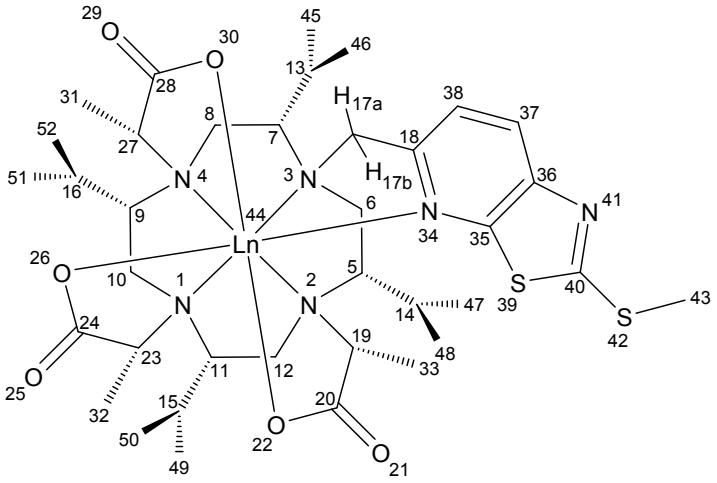

Lanthanide trifluoromethanesulfonate (2.0 eq.) was added to (2*R*,2'*R*,2''*R*)-2,2',2''-((2*S*,5*S*,8*S*,11*S*)-2,5,8,11-tetraisopropyl-10-((2-(methylthio)thiazolo[5,4-*b*]pyridin-5-yl)methyl)-1,4,7,10-tetraazacyclododecane-1,4,7-triyl)tripropionic acid (1.0 eq.) in aq. ammonium acetate (10 ml, 100 mM) and stirred overnight at 80 °C. The solvent was evaporated and the residue was subjected to preparative HPLC to give Ln-(2*R*,2'*R*,2''*R*)-2,2',2''-((2*S*,5*S*,8*S*,11*S*)-2,5,8,11-tetraisopropyl-10-((2-(methylthio)thiazolo[5,4-*b*]pyridin-5-yl)methyl)-1,4,7,10-tetraazacyclododecane-1,4,7-triyl)tripropionate as white powders (Lutetium: 12 mg, 75.1%, Thulium: 10 mg, 63.0%, Dysprosium: 7 mg, 44.4%).

Λ(δδδδ)-Lu-P4T-DOTA$_{red}$

^{1}H NMR (600 MHz, Deuterium Oxide, pH 6.0) δ 8.25 (d, J = 8.5 Hz, 1H, H37), 7.54 (d, J = 8.5 Hz, 1H, H38), 4.70 (d, J = 17.5 Hz, 1H, H17b), 4.43 (d, J = 17.4 Hz, 1H, H17a), 3.84 (q, J = 7.4 Hz, 1H, H27), 3.76 (q, J = 7.3 Hz, 1H, H23), 3.47 (dd, J = 13.7, 13.7 Hz, H6ax), 3.18 - 3.06 (m, 2H, H8eq,8ax), 3.06 - 2.98 (m, 3H, H12ax,10eq,10ax), 2.98 - 2.92 (m, 3H, H7,12eq,6eq), 2.88 - 2.84 (m, 1H, H9), 2.81 (q, J = 7.0 Hz, 3H, H19), 2.78 (s, 3H, H43), 2.71 - 2.65 (m, 2H, H5,11), 2.54 - 2.47 (m, 2H, H15,16), 2.47 - 2.41 (m, 1H, H13), 2.37 - 2.30 (m, 1H, H14), 1.59 (d, J = 7.2 Hz, 3H, H32), 1.58 (d, J = 7.2 Hz, 3H, H31), 1.30 (d, J = 7.0 Hz, 3H, H33), 1.12 (d, J = 7.1 Hz, 3H, H46), 1.10 (d, J = 6.8 Hz, 3H, H45), 1.07 (d, J = 7.1 Hz, 3H, H52), 1.04 (d, J = 7.1 Hz, 3H, H51), 1.03 (d, J = 7.5 Hz, 3H, H50), 1.01 (d, J = 6.8 Hz, 3H, H49), 0.95 (d, J = 6.8 Hz, 3H, H47), 0.84 (d, J = 6.9 Hz, 3H, H48).

^{13}C NMR (151 MHz, Deuterium Oxide, pH 6.0, TSP-d_4, extracted from HMQC and HMBC) δ 186.1 (C28), 185.8 (C24), 185.4 (C20), 177.6 (C40), 158.7 (C35), 158.7 (C18), 150.5 (C36), 134.4 (C37), 123.0 (C38), 73.4 (C7), 73.1 (C11), 73.1 (C9), 72.8 (C5), 71.1 (C23), 70.9 (C27), 69.6 (C19), 67.7 (C17), 53.1 (C6), 45.1 (C10), 44.8 (C8), 44.4 (C12), 29.9 (C16), 29.9 (C15), 29.4 (C14), 27.4 (C13), 26.7 (C50), 26.7 (C46), 26.5 (C52), 25.3 (C48), 20.4 (C45), 20.0 (C49), 20.0 (C47), 20.0 (C51), 18.2 (C43), 17.0 (C31), 16.7 (C32), 16.2 (C33).

Ln = Lu, HRMS: $[M+H]^+$, $C_{37}H_{60}LuN_6O_6S_2$, m/z (calc.) = 923.3418, m/z (meas.) = 923.3418.
Ln = Tm, HRMS: $[M+H]^+$, $C_{37}H_{60}N_6O_6S_2Tm$, m/z (calc.) = 917.3352, m/z (meas.) = 917.3356.
Ln = Dy, HRMS: $[M+H]^+$, $C_{37}H_{60}DyLuN_6O_6S_2$, m/z (calc.) = 912.3302, m/z (meas.) = 912.3302.

Λ(δδδδ)-Ln-(2*R*,2'*R*,2''*R*)-2,2',2''-((2*S*,5*S*,8*S*,11*S*)-2,5,8,11-tetraisopropyl-10-((2-(methylsulfonyl)thiazolo[5,4-*b*]pyridin-5-yl)methyl)-1,4,7,10-tetraazacyclododecane-1,4,7-triyl)tripropionate, Ln-P4T-DOTA

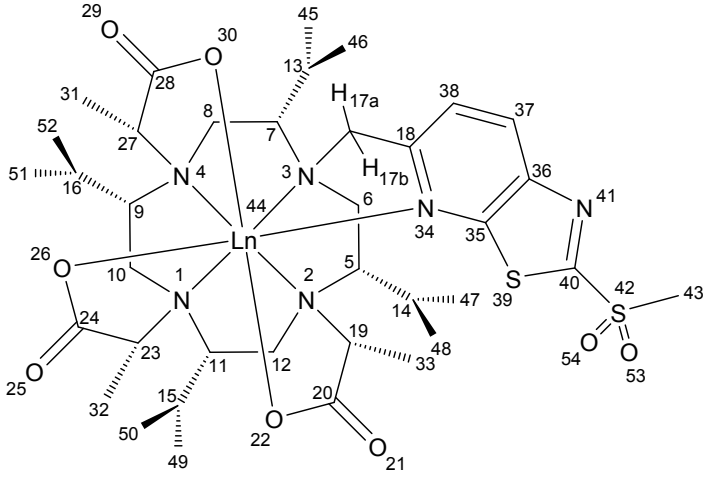

meta-Chloroperbenzoic acid (10.0 eq.) was added to Ln-(2*R*,2'*R*,2''*R*)-2,2',2''-((2*S*,5*S*,8*S*,11*S*)-2,5,8,11-tetraisopropyl-10-((2-(methylthio)thiazolo[5,4-*b*]pyridin-5-yl)methyl)-1,4,7,10-tetraazacyclododecane-1,4,7-triyl)tripropionate (1.0 eq.) in DCM (10 ml) and the mixture was stirred overnight at rt. Then *meta*-chloroperbenzoic acid (10.0 eq.) was added and the mixture was stirred for 3 h at rt. The mixture was washed with sodium bicarbonate and the organic phase was subjected to preparative HPLC to give Λ(δδδδ)-Ln-(2*R*,2'*R*,2''*R*)-2,2',2''-((2*S*,5*S*,8*S*,11*S*)-2,5,8,11-tetraisopropyl-10-((2-(methylsulfonyl)thiazolo[5,4-*b*]pyridin-5-yl)methyl)-1,4,7,10-tetraazacyclododecane-1,4,7-triyl)tripropionate as white powders (Lutetium: 3.5 mg, 28.2%, Thulium: 3.2 mg, 28.0%, Dysprosium: 2.5 mg, 34.5%). Solutions of Ln-P4T-DOTA were stored in dry acetonitrile after purification by preparative HPLC.

Λ(δδδδ)-Lu-P4T-DOTA

^{1}H NMR (600 MHz, Deuterium Oxide, pH 6.0) δ 8.73 (d, J = 8.7 Hz, 1H, H37), 7.81 (d, J = 8.8 Hz, 1H, H38), 4.87 (d, J = 18.7 Hz, 1H, H17b), 4.60 (d, J = 18.5 Hz, 1H, H17a), 3.85 (q, J = 7.5 Hz, 1H, H27), 3.78 (q, J = 7.7 Hz, 1H, H23), 3.56 - 3.48 (m, H43,6ax), 3.18 - 3.07 (m, 3H, H8ax,10eq,12ax), 3.07 - 3.01 (m, 2H, H10ax,12eq), 3.01 - 2.91 (m, 4H, H7,8eq,6eq,19), 2.90 - 2.84 (m, 1H, H9), 2.71 - 2.68 (m, 1H, H11), 2.67 - 2.64 (m, 1H, H5), 2.55 - 2.41 (m, 3H, H15,16,13), 2.41 - 2.30 (m, 1H, H14), 1.60 (d, J = 7.4 Hz, 3H, H32), 1.57 (d, J = 7.3 Hz, 3H, H31), 1.32 (d, J = 7.1 Hz, 3H, H33), 1.13 (d, J = 7.4 Hz, 3H, H46), 1.11 (d, J = 6.9 Hz, 3H, H45), 1.07 (d, J = 7.1 Hz, 3H, H52), 1.04 (d, J = 6.4 Hz, 3H, H51), 1.03 (d, J = 6.7 Hz, 3H, H50), 1.01 (d, J = 6.8 Hz, 3H, H49), 0.96 (d, J = 6.7 Hz, 3H, H47), 0.85 (d, J = 6.9 Hz, 3H, H48).

^{13}C NMR (151 MHz, Deuterium Oxide, pH 6.0, TSP-d_4, extracted from HMQC and HMBC) δ 186.3 (C28), 185.7 (C24), 185.4 (C20), 174.7 (C40), 164.7 (C18), 158.9 (C35), 149.7 (C36), 140.1 (C37), 125.1 (C38), 73.6 (C7), 73.4 (C11), 73.3 (C9), 73.2 (C5), 71.3 (C23), 71.0 (C27), 69.8 (C19), 68.3 (C17), 53.4 (C6), 45.2 (C12), 45.0 (C43), 45.0 (C10), 44.6 (C8), 30.0 (C16), 30.0 (C15), 29.5 (C14), 27.7 (C13), 26.7 (C46), 26.6 (C52), 25.4 (C48), 20.4 (C45), 20.1 (C47), 20.1 (C50), 20.1 (C49), 17.1 (C32), 17.1 (C31), 16.4 (C33).

Ln = Lu, HRMS: $[M+H]^+$, $C_{37}H_{60}LuN_6O_8S_2$, m/z (calc.) = 955.3316, m/z (meas.) = 955.3322.

Ln = Tm, HRMS: $[M+H]^+$, $C_{37}H_{60}N_6O_8S_2Tm$, m/z (calc.) = 949.3251, m/z (meas.) = 949.3266.

Ln = Dy, HRMS: $[M+H]^+$, $C_{37}H_{60}DyLuN_6O_8S_2$, m/z (calc.) = 944.3200, m/z (meas.) = 944.3210.

^{1}H-NMR of Lu-P4T-DOTA$_{red}$

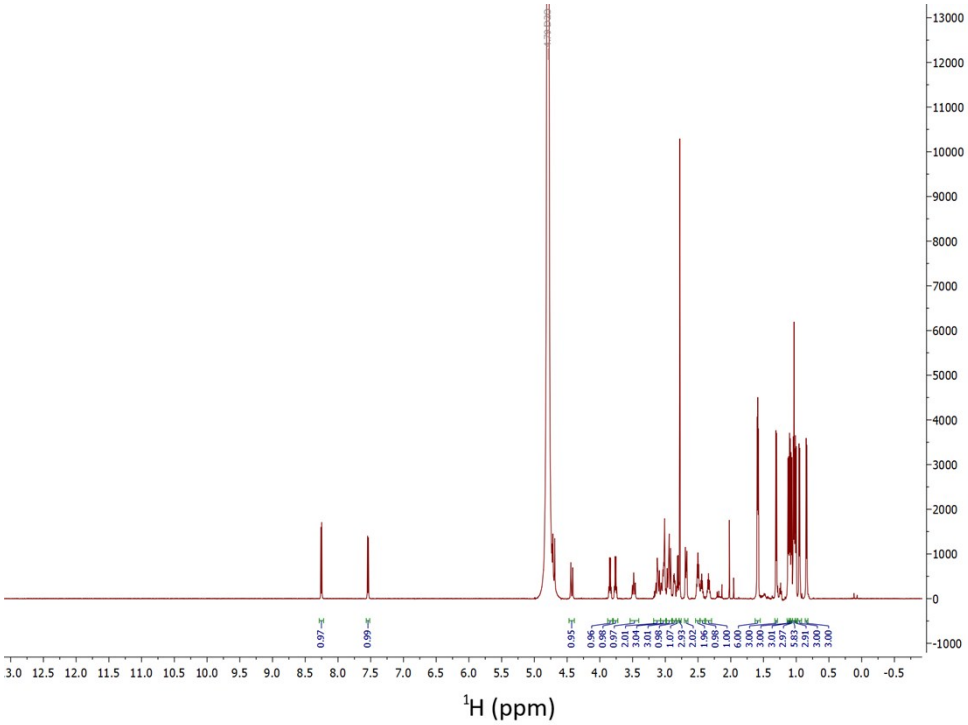

Figure S1: ^{1}H-NMR of Lu-P4T-DOTA$_{red}$ in D_2O (pH 6.0) at 298 K.

^{1}H-NMR of Lu-P4T-DOTA

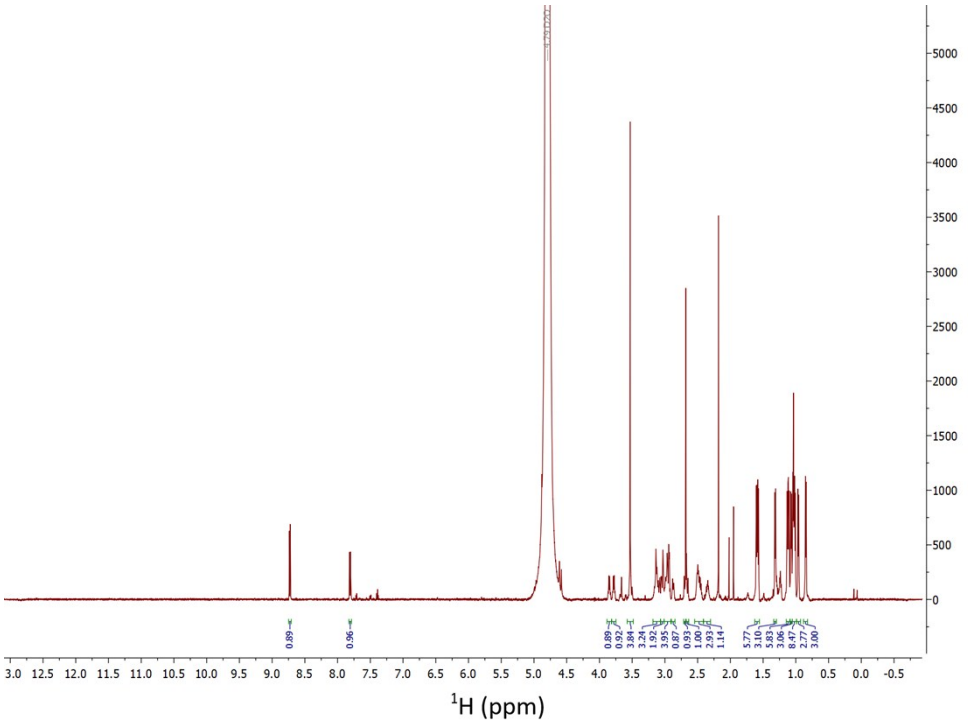

Figure S2: ^{1}H-NMR of Lu-P4T-DOTA in D_2O (pH 6.0) at 298 K.

^{1}H-NMR of Tm-P4T-DOTA

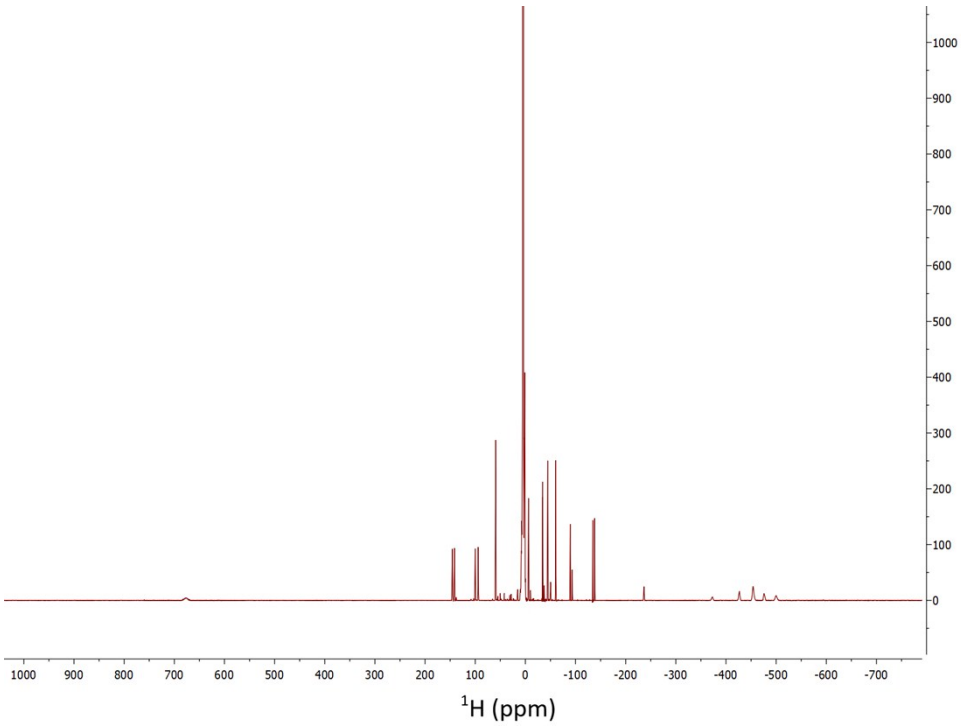

Figure S3: ^{1}H-NMR of Tm-P4T in D_2O at 298 K.

^{1}H-NMR of Dy-P4T-DOTA

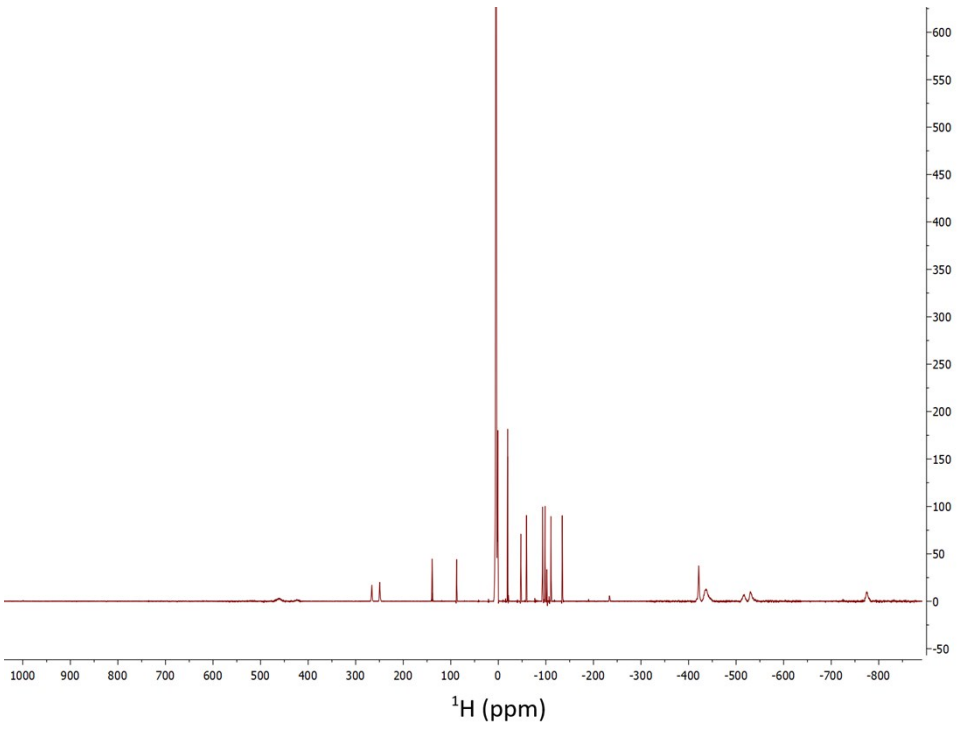

Figure S4: ^{1}H-NMR of Dy-P4T in D_2O at 298 K.

HPLC measurements of Ln-P4T

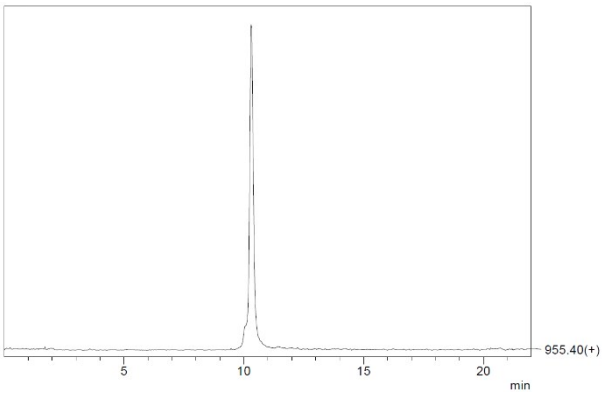

Figure S5: HPLC-MS trace of Lu-P4T.

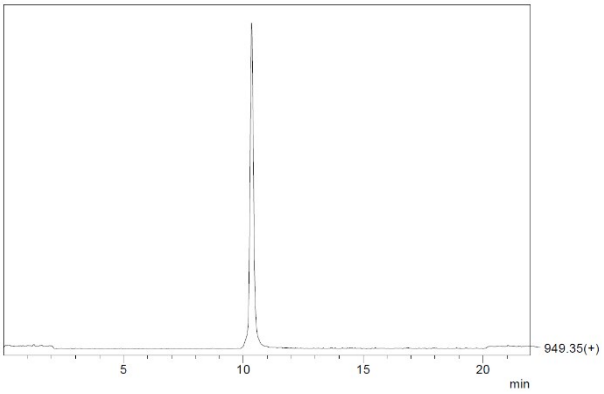

Figure S6: HPLC-MS trace of Tm-P4T.

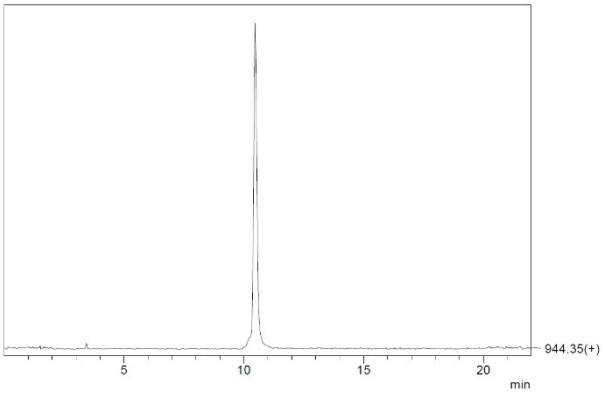

Figure S7: HPLC-MS trace of Dy-P4T.

Overlay of ^{1}H-^{15}N HSQC spectra of Dy-P4T-Ub^{S57C} (blue), Tm-P4T-Ub^{S57C} (red) and Lu-P4T-Ub^{S57C} (black)

Measured in 10 mM phosphate buffer with pH 6.0 at a temperature of 298 K on a 600 MHz Bruker Avance III NMR spectrometer equipped with a cryogenic QCI-F probe.

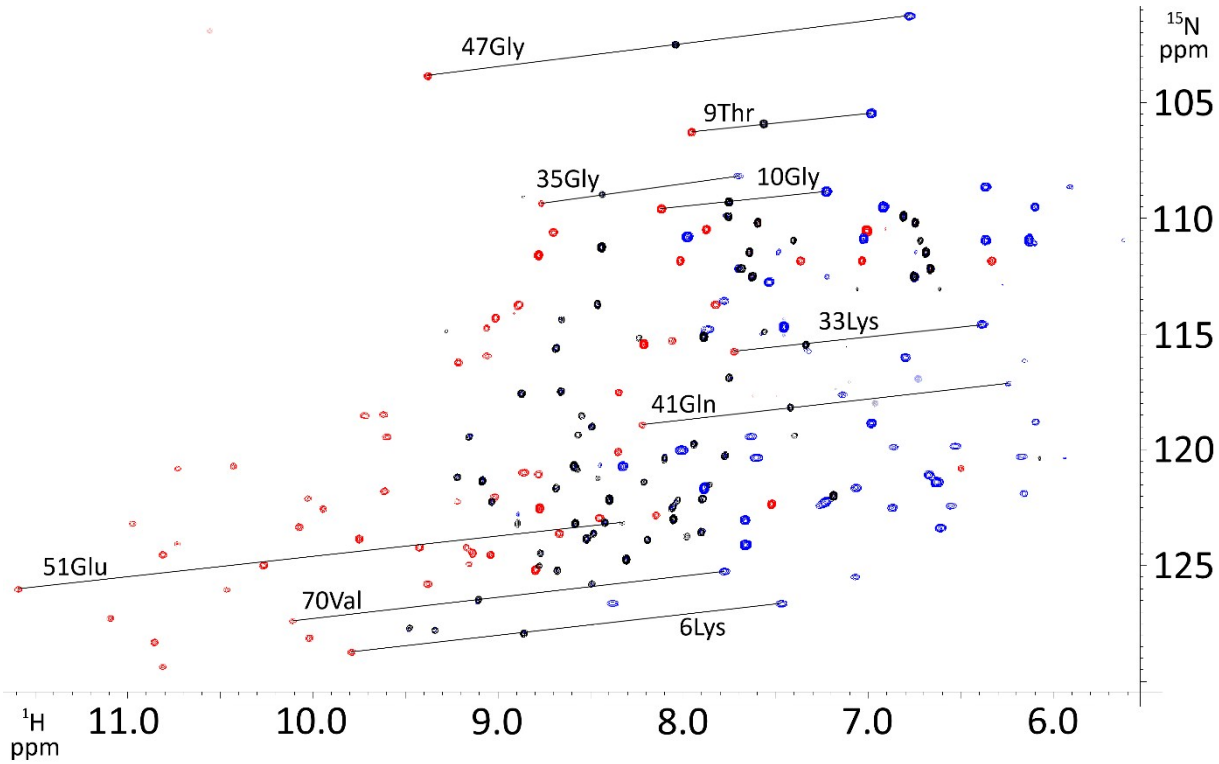

Figure S8: Overlay of ^{1}H-^{15}N HSQC spectra of Dy-P4T-Ub^{S57C} (blue), Tm-P4T-Ub^{S57C} (red) and Lu-P4T-Ub^{S57C} (black).

Overlay of ^{1}H-^{15}N HSQC spectra of Dy-P4T-Ub^{K48C} (blue), Tm-P4T-Ub^{K48C} (red) and Lu-P4T-Ub^{K48C} (black) attached to ubiquitin K48C

Measured in 10 mM phosphate buffer with pH 6.0 at a temperature of 298 K on a 600 MHz Bruker Avance III NMR spectrometer equipped with a cryogenic QCI-F probe.

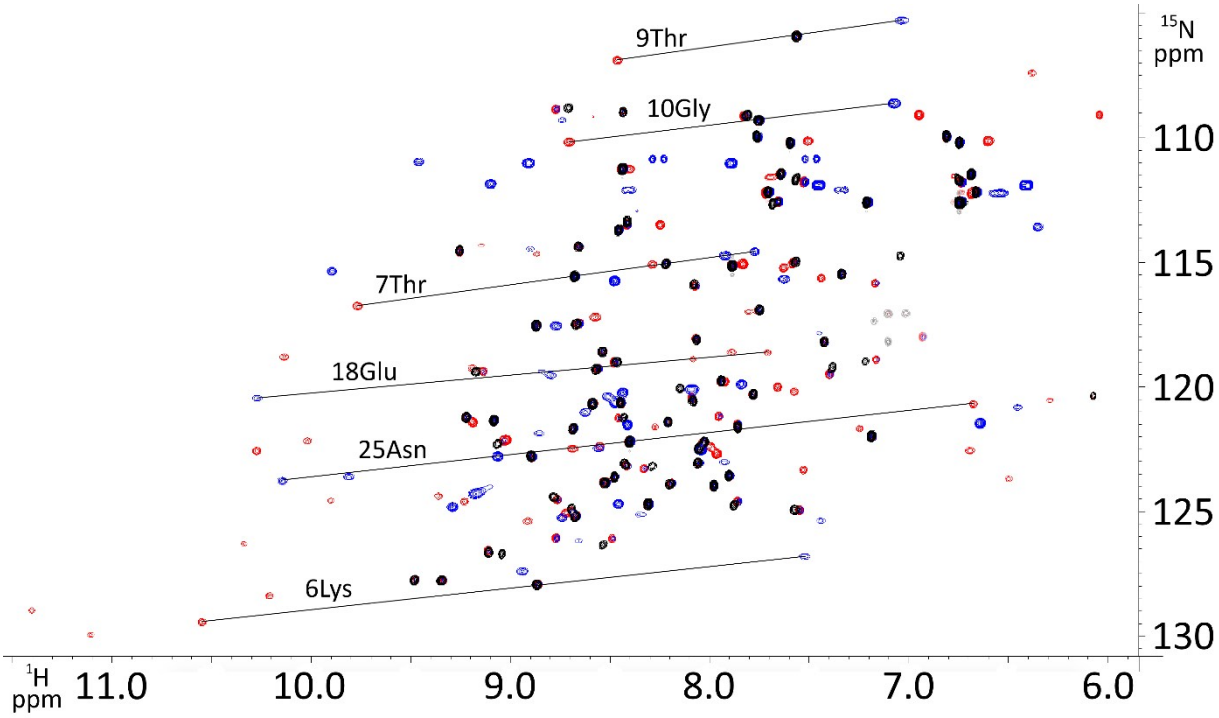

Figure S9: Overlay of ^{1}H-^{15}N HSQC spectra of Dy-P4T-Ub^{K48C} (blue), Tm-P4T-Ub^{K48C} (red) and Lu-P4T-Ub^{K48C} (black).

Overlay of ^{1}H-^{15}N HSQC spectra of Dy-P4T (blue), Tm-P4T (red) and Lu-P4T (black) attached to selectively ^{15}N leucine labeled hCA II S166C

Measured in 10 mM phosphate buffer with pH 6.8 at a temperature of 298 K on a 600 MHz Bruker Avance III NMR spectrometer equipped with a cryogenic QCI-F probe.

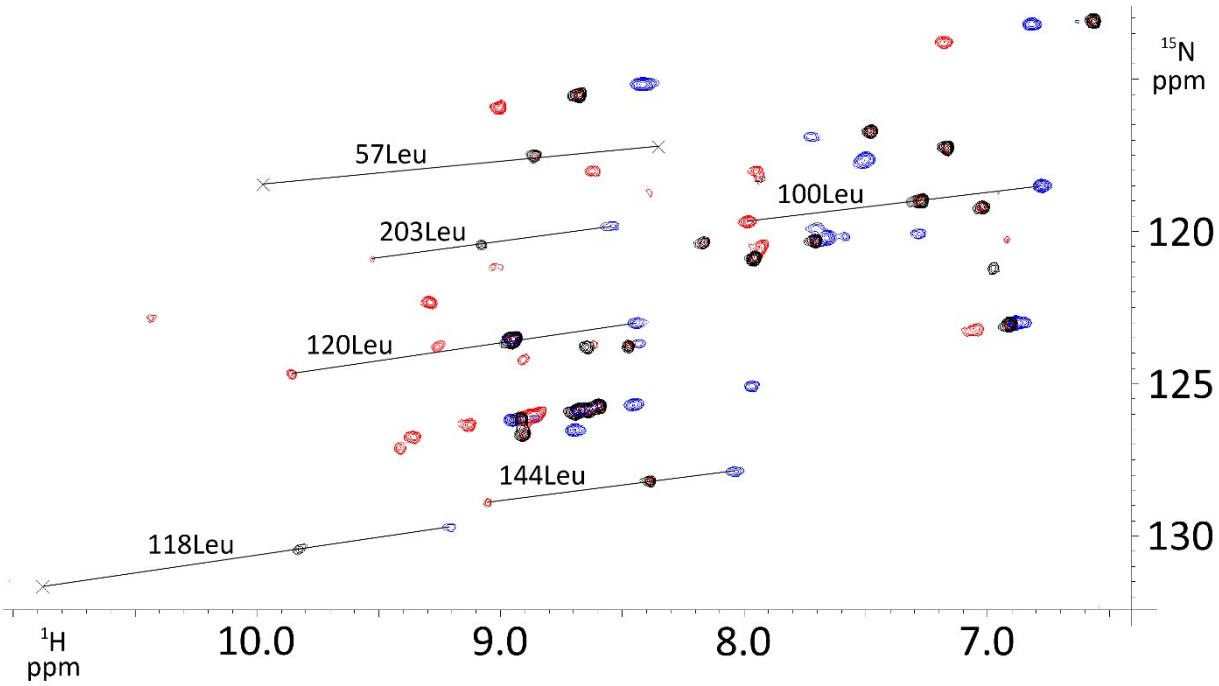

Figure S10: Overlay of ^{1}H-^{15}N HSQC spectra of Dy-P4T (blue), Tm-P4T (red) and Lu-P4T (black) attached to selectively ^{15}N leucine labeled hCA II S166C.

Shift list comparison of ^{1}H-^{15}N HSQC spectra of Dy- and Lu-P4T-Ub^{S57C}

Table S1: Shift list comparison of ^{1}H-^{15}N HSQC spectra of Dy- and Lu-P4T-Ub^{S57C}.

Residue	Reson. 1	Shift Dy	Shift Lu	Reson. 2		Shift Dy	Shift Lu
2Gln	H	6.18	8.89	N		120.31	123.17
4Phe	H	6.16	8.55	N		116.17	118.53
5Val	H	7.63	9.22	N		119.43	121.19
6Lys	H	7.47	8.86	N		126.64	127.93
12Thr	H	8.01	8.59	N		120.02	120.71
13Ile	H	8.38	9.48	N		126.63	127.69
14Thr	H	7.61	8.69	N		120.35	121.66
15Leu	H	6.61	8.68	N		123.37	125.22
28Ala	H	6.16	7.90	N		121.88	123.56
29Lys	H	6.10	7.77	N		118.80	120.26
30Ile	H	6.53	8.21	N		119.84	121.39
31Gln	H	7.23	8.48	N		122.27	123.61
32Asp	H	6.98	7.94	N		118.85	119.76
33Lys	H	6.39	7.34	N		114.59	115.46
34Glu	H	7.78	8.66	N		113.56	114.38
39Asp	H	7.54	8.46	N		112.76	113.72
40Gln	H	6.80	7.75	N		116.01	116.90
41Gln	H	6.24	7.42	N		117.14	118.18
42Arg	H	7.06	8.42	N		121.65	123.15
43Leu	H	6.55	8.77	N		122.43	124.47
44Ile	H	6.86	9.03	N		119.88	122.25
49Gln	H	6.67	8.58	N		121.08	123.19
67Leu	H	7.07	9.34	N		125.49	127.80
69Leu	H	6.87	8.19	N		122.50	123.88
70Val	H	7.78	9.11	N		125.26	126.48

Shift list comparison of ^{1}H-^{15}N HSQC spectra of Tm- and Lu-P4T-Ub^{S57C}

Table S2: Shift list comparison of ^{1}H-^{15}N HSQC spectra of Tm- and Lu-P4T-Ub^{S57C}.

Residue	Reson. 1	Shift Tm	Shift Lu	Reson. 2	Shift Tm	Shift Lu
3Ile	H	9.06	8.24	N	115.95	115.17
4Phe	H	9.60	8.55	N	119.45	118.53
5Val	H	10.03	9.22	N	122.11	121.19
6Lys	H	9.79	8.86	N	128.74	127.93
7Thr	H	9.21	8.69	N	116.23	115.63
12Thr	H	8.86	8.59	N	120.99	120.71
13Ile	H	10.02	9.48	N	128.14	127.69
14Thr	H	9.02	8.69	N	122.07	121.66
15Leu	H	9.38	8.68	N	125.80	125.22
16Glu	H	8.45	8.06	N	122.94	122.50
23Ile	H	13.34	8.46	N	125.72	121.22
25Asn	H	10.07	7.86	N	123.34	121.51
26Val	H	10.81	8.03	N	124.53	122.21
27Lys	H	10.43	8.49	N	120.72	119.00
28Ala	H	9.04	7.90	N	124.54	123.56
29Lys	H	8.78	7.77	N	121.06	120.26
30Ile	H	9.22	8.21	N	122.24	121.39
31Gln	H	9.17	8.48	N	124.22	123.61
32Asp	H	8.35	7.94	N	120.09	119.76
33Lys	H	7.72	7.34	N	115.76	115.46
34Glu	H	9.06	8.66	N	114.75	114.38
39Asp	H	9.01	8.46	N	114.31	113.72
40Gln	H	8.35	7.75	N	117.53	116.90
41Gln	H	8.22	7.42	N	118.93	118.18
42Arg	H	9.42	8.42	N	124.22	123.15
43Leu	H	10.46	8.77	N	126.05	124.47
44Ile	H	10.73	9.03	N	124.06	122.25
45Phe	H	11.09	8.78	N	127.28	125.01
48Lys	H	9.75	7.90	N	123.86	122.12
49Gln	H	10.26	8.58	N	124.99	123.19
66Thr	H	9.72	8.66	N	118.54	117.48
67Leu	H	10.81	9.34	N	129.38	127.80
68His	H	10.73	9.16	N	120.82	119.45
69Leu	H	9.15	8.66	N	124.93	123.87
70Val	H	10.11	9.11	N	127.40	126.48
71Leu	H	8.67	8.05	N	123.62	123.00

Shift list comparison of ^{1}H-^{15}N HSQC spectra of Dy- and Lu-P4T-Ub^{K48C}

Table S3: Shift list comparison of ^{1}H-^{15}N HSQC spectra of Dy- and Lu-P4T-Ub^{K48C}.

Residue	Reson. 1	Shift Dy	Shift Lu	Reson. 2	Shift Dy	Shift Lu
2Gln	H	8.56	8.89	N	122.46	122.78
3Ile	H	7.92	8.22	N	114.73	115.07
5Val	H	8.44	9.22	N	120.22	121.22
6Lys	H	7.52	8.87	N	126.81	127.94
7Thr	H	7.77	8.68	N	114.57	115.56
13Ile	H	8.94	9.48	N	127.41	127.76
14Thr	H	8.45	8.68	N	121.25	121.68
27Lys	H	8.80	8.46	N	119.53	119.00
30Ile	H	8.41	8.21	N	121.53	121.41
32Asp	H	8.09	7.94	N	120.10	119.76
33Lys	H	7.63	7.34	N	115.67	115.47
39Asp	H	8.90	8.46	N	114.46	113.71
40Gln	H	8.77	7.75	N	117.55	116.91
42Arg	H	9.17	8.43	N	124.29	123.08
70Val	H	8.66	9.11	N	126.18	126.65

Shift list comparison of ^{1}H-^{15}N HSQC spectra of Tm- and Lu-P4T-Ub^{K48C}

Table S4: Shift list comparison of ^{1}H-^{15}N HSQC spectra of Tm- and Lu-P4T-Ub^{K48C}.

Residue	Reson. 1	Shift Tm	Shift Lu	Reson. 2	Shift Tm	Shift Lu
2Gln	H	8.69	8.89	N	122.48	122.78
3Ile	H	8.29	8.22	N	115.08	115.07
5Val	H	10.02	9.22	N	122.17	121.22
6Lys	H	10.55	8.87	N	129.44	127.94
7Thr	H	9.77	8.68	N	116.75	115.56
12Thr	H	9.19	8.59	N	121.43	120.68
13Ile	H	10.21	9.48	N	128.39	127.76
25Asn	H	6.68	7.86	N	120.69	121.62
26Val	H	7.25	8.03	N	121.68	122.23
27Lys	H	8.08	8.46	N	118.88	119.00
28Ala	H	7.53	7.90	N	123.33	123.56
29Lys	H	7.57	7.78	N	120.19	120.30
30Ile	H	8.27	8.21	N	121.60	121.41
33Lys	H	7.44	7.34	N	115.64	115.47
34Glu	H	8.87	8.66	N	114.67	114.38
39Asp	H	8.25	8.44	N	113.49	113.53
40Gln	H	7.81	7.75	N	116.98	116.91
41Gln	H	7.89	7.42	N	118.61	118.19
42Arg	H	9.90	8.43	N	124.56	123.08
43Leu	H	11.57	8.78	N	127.37	124.43
44Ile	H	13.95	9.06	N	128.26	122.29
66Thr	H	10.14	8.67	N	118.80	117.48
67Leu	H	11.11	9.34	N	129.95	127.77
68His	H	13.29	9.17	N	122.85	119.40
69Leu	H	10.34	8.20	N	126.31	123.90
70Val	H	11.40	9.11	N	128.98	126.65
71Leu	H	9.36	8.06	N	124.38	123.06

Shift list comparison of ^{1}H-^{15}N HSQC spectra of Dy- and Lu-P4T attached to selectively ^{15}N leucine labelled hCA II S166C

Table S5: Shift list comparison of ^{1}H-^{15}N HSQC spectra of Dy- and Lu-P4T attached to selectively ^{15}N leucine labelled hCA II S166C.

Residue	Reson. 1	Shift Dy	Shift Lu	Reson. 2	Shift Dy	Shift Lu
47Leu	H	8.41	8.68	N	115.17	115.53
57Leu	H	6.82	6.56	N	113.19	113.10
79Leu	H	7.72	7.48	N	116.90	116.72
84Leu	H	7.51	7.17	N	117.67	117.26
90Leu	H	6.78	7.27	N	118.51	119.01
100Leu	H	8.35	8.86	N	117.23	117.52
118Leu	H	8.54	9.08	N	119.83	120.44
120Leu	H	8.97	8.95	N	123.50	123.55
141Leu	H	8.44	8.95	N	123.02	123.56
144Leu	H	8.43	8.47	N	123.69	123.77
148Leu	H	9.21	9.83	N	129.72	130.44
157Leu	H	8.03	8.39	N	127.89	128.21
184Leu	H	7.49	7.93	N	117.67	118.30
185Leu	H	7.71	8.16	N	119.90	120.36
198Leu	H	8.70	8.91	N	126.53	126.65
203Leu	H	7.97	8.59	N	125.09	125.74
212Leu	H	8.45	8.64	N	125.71	125.86
224Leu	H	7.28	7.96	N	120.09	120.88
240Leu	H	7.66	7.71	N	120.21	120.32
251Leu	H	8.95	8.91	N	126.20	126.17

Shift list comparison of ^{1}H-^{15}N HSQC spectra of Tm- and Lu-P4T attached to selectively ^{15}N leucine labelled hCA II S166C

Table S6: Shift list comparison of ^{1}H-^{15}N HSQC spectra of Tm- and Lu-P4T attached to selectively ^{15}N leucine labelled hCA II S166C.

Residue	Reson. 1	Shift Tm	Shift Lu	Reson. 2	Shift Tm	Shift Lu
44Leu	H	7.06	6.91	N	123.24	123.06
47Leu	H	9.13	8.91	N	126.37	126.17
57Leu	H	9.98	8.86	N	118.47	117.52
79Leu	H	9.26	8.95	N	123.81	123.55
84Leu	H	7.93	7.71	N	120.54	120.32
90Leu	H	8.91	8.47	N	124.25	123.77
100Leu	H	7.98	7.27	N	119.69	119.01
118Leu	H	10.88	9.83	N	131.67	130.44
120Leu	H	9.86	8.95	N	124.69	123.56
141Leu	H	9.00	8.68	N	115.94	115.53
144Leu	H	9.05	8.39	N	128.90	128.21
148Leu	H	9.03	8.16	N	121.17	120.36
157Leu	H	8.63	7.48	N	118.02	116.72
184Leu	H	7.95	7.17	N	118.04	117.26
185Leu	H	7.18	6.56	N	113.79	113.10
189Leu	H	8.87	8.69	N	126.06	125.92
198Leu	H	8.39	7.93	N	118.72	118.30
203Leu	H	9.53	9.08	N	120.91	120.44
212Leu	H	9.42	8.91	N	127.12	126.65
224Leu	H	9.29	7.96	N	122.33	120.88
229Leu	H	10.44	7.02	N	122.85	119.20
240Leu	H	9.36	8.59	N	126.75	125.74
251Leu	H	8.84	8.64	N	125.95	125.86

Residual dipolar couplings measured in ^{1}H-^{15}N HSQC spectra of Dy- and Lu-P4T-Ub^{S57C}

Table S7: Residual dipolar couplings measured in ^{1}H-^{15}N HSQC spectra of Dy- and Lu-P4T-Ub^{S57C}.

Residue	RDC (Hz)
2	9.5
4	1.8
5	1.2
6	5.1
12	-1.1
13	-0.6
14	5.5
15	-3.9
28	11.1
29	11.4
30	5.8
32	14.3
33	8.7
34	5.7
39	-8.4
40	-4.5
41	-28.5
42	-8.3
43	-8.6
44	1.3
49	-0.5
67	-3.8
69	-5.1
70	-11.1

Residual dipolar couplings measured in ^{1}H-^{15}N HSQC spectra of Tm- and Lu-P4T-Ub^{S57C}

Table S8: Residual dipolar couplings measured in ^{1}H-^{15}N HSQC spectra of Tm- and Lu-P4T-Ub^{S57C}.

Residue	RDC (Hz)
3	12.7
4	9.9
5	6.3
6	5.5
7	2.4
12	3.6
13	3.2
14	8.0
15	11.6
16	7.9
23	8.6
25	1.6
26	5.5
27	5.9
28	-6.9
29	9.4
30	6.0
31	1.4
32	-0.5
33	5.0
34	3.6
39	14.1
40	-4.8
41	5.6
42	3.0
43	7.1
44	4.1
45	2.8
48	-14.7
49	-2.9
66	11.9
67	4.5
68	5.9
69	8.2
70	2.0
71	2.6

Correlation plots of experimental and back-calculated PCS and RDC

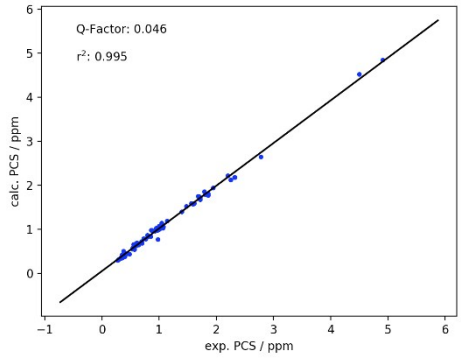

Figure S11: PCS correlation plot of ^{15}N labelled ubiquitin S57C labelled with Tm-P4T-DOTA.

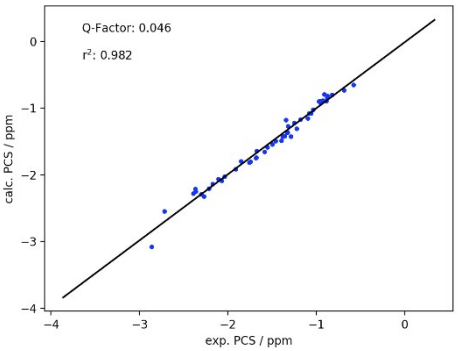

Figure S12: PCS correlation plot of ^{15}N labelled ubiquitin S57C labelled with Dy-P4T-DOTA.

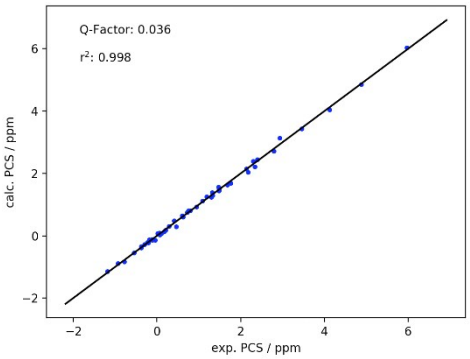

Figure S13: PCS correlation plot of ^{15}N labelled ubiquitin K48C labelled with Tm-P4T-DOTA.

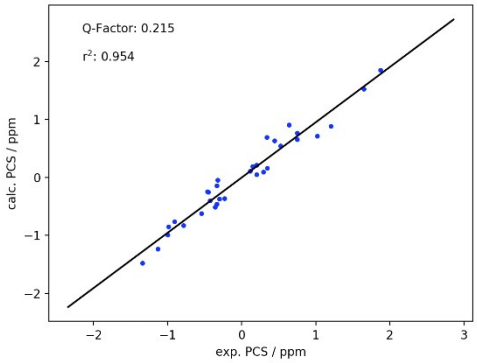

Figure S14: PCS correlation plot of ^{15}N labelled ubiquitin K48C labelled with Dy-P4T-DOTA.

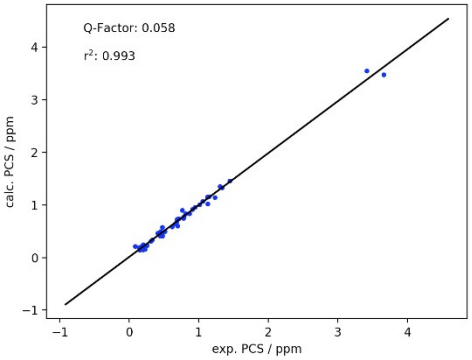

Figure S15: PCS correlation plot of selectively ^{15}N leucine labelled hCA S166C labelled with Tm-P4T-DOTA.

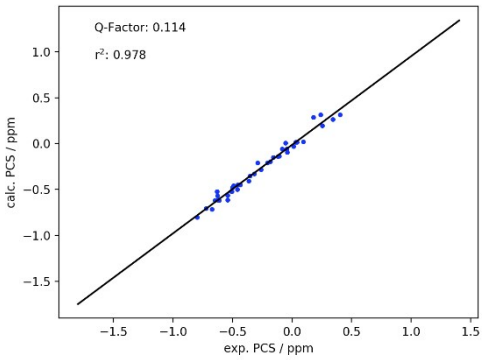

Figure S16: PCS correlation plot of selectively ^{15}N leucine labelled hCA S166C labelled with Dy-P4T-DOTA.

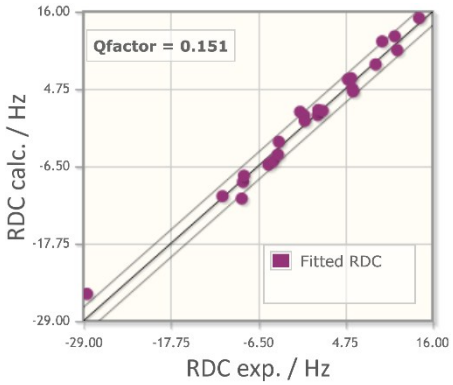

Figure S17: RDC correlation plot of ^{15}N labelled ubiquitin S57C labelled with Tm-P4T-DOTA.

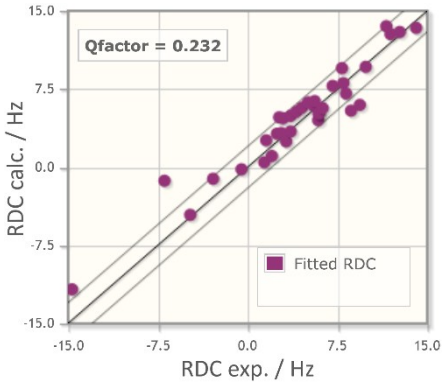

Figure S18: RDC correlation plot of ^{15}N labelled ubiquitin S57C labelled with Dy-P4T-DOTA.

DFT calculations of the Ln-P4T complexes in vacuo and water solvent

For the calculations, BP86 was used as functional,[10-11] SARC-TZVP as basis set for the ligands,[12] while SARC2-QZVP was used as basis set for the lanthanide metal.[13] The calculations were performed using the relativistic ZORA approximation,[14] as well as the RI approximation to speed up the calculations.[15-16] To model the water solvent, CPCM solvent model was implemented into the calculations.[17]

References

1. Sass, J.; Cordier, F.; Hoffmann, A.; Rogowski, M.; Cousin, A.; Omichinski, J. G.; Löwen, H.; Grzesiek, S., Purple Membrane Induced Alignment of Biological Macromolecules in the Magnetic Field. *JACS* **1999,** *121* (10), 2047-2055.
2. Varghese, S.; Halling, P. J.; Häussinger, D.; Wimperis, S., High-Resolution Structural Characterization of a Heterogeneous Biocatalyst Using Solid-State NMR. *J. Phys. Chem. C* **2016,** *120* (50), 28717-28726.
3. Vranken, W. F.; Boucher, W.; Stevens, T. J.; Fogh, R. H.; Pajon, A.; Llinas, M.; Ulrich, E. L.; Markley, J. L.; Ionides, J.; Laue, E. D., The CCPN data model for NMR spectroscopy: Development of a software pipeline. *Proteins: Struct., Funct., Bioinf.* **2005,** *59* (4), 687-696.
4. Ramage, R.; Green, J.; Muir, T. W.; Ogunjobi, O. M.; Love, S.; Shaw, K., Synthetic, structural and biological studies of the ubiquitin system: the total chemical synthesis of ubiquitin. *Biochem. J* **1994,** *299 (Pt 1)*, 151-8.
5. Maltsev, A. S.; Grishaev, A.; Roche, J.; Zasloff, M.; Bax, A., Improved Cross Validation of a Static Ubiquitin Structure Derived from High Precision Residual Dipolar Couplings Measured in a Drug-Based Liquid Crystalline Phase. *JACS* **2014,** *136* (10), 3752-3755.
6. Avvaru, B. S.; Kim, C. U.; Sippel, K. H.; Gruner, S. M.; Agbandje-McKenna, M.; Silverman, D. N.; McKenna, R., A short, strong hydrogen bond in the active site of human carbonic anhydrase II. *Biochemistry* **2010,** *49* (2), 249-51.
7. Schmitz, C.; Stanton-Cook, M. J.; Su, X.-C.; Otting, G.; Huber, T., Numbat: an interactive software tool for fitting Δχ-tensors to molecular coordinates using pseudocontact shifts. *J. Biomol. NMR* **2008,** *41* (3), 179.
8. Joss, D.; Bertrams, M.-S.; Häussinger, D., A sterically overcrowded, isopropyl-substituted lanthanide chelating tag for protein PCS NMR spectroscopy: Synthesis of its macrocyclic scaffold and benchmarking on ubiquitin S57C and hCA II S166C. *Chem. Eur. J.* **2019**, *in press*, DOI:10.1002/chem.201901692.
9. Müntener, T.; Kottelat, J.; Huber, A.; Häussinger, D., New Lanthanide Chelating Tags for PCS NMR Spectroscopy with Reduction Stable, Rigid Linkers for Fast and Irreversible Conjugation to Proteins. *Bioconjugate Chem.* **2018,** *29* (10), 3344-3351.
10. Becke, A. D., Density-functional exchange-energy approximation with correct asymptotic behavior. *Phys. Rev. A* **1988,** *38* (6), 3098-3100.
11. Perdew, J. P., Density-functional approximation for the correlation energy of the inhomogeneous electron gas. *Phys. Rev. B* **1986,** *33* (12), 8822-8824.
12. Pantazis, D. A.; Neese, F., All-Electron Scalar Relativistic Basis Sets for the Lanthanides. *J. Chem. Theory Comput.* **2009,** *5* (9), 2229-2238.
13. Aravena, D.; Neese, F.; Pantazis, D. A., Improved Segmented All-Electron Relativistically Contracted Basis Sets for the Lanthanides. *J. Chem. Theory Comput.* **2016,** *12* (3), 1148-1156.
14. Lenthe, E. v.; Baerends, E. J.; Snijders, J. G., Relativistic regular two-component Hamiltonians. *J. Chem. Phys.* **1993,** *99* (6), 4597-4610.
15. Kendall, R. A.; Früchtl, H. A., The impact of the resolution of the identity approximate integral method on modern ab initio algorithm development. *Theor. Chem. Acc.* **1997,** *97* (1), 158-163.
16. Vahtras, O.; Almlöf, J.; Feyereisen, M. W., Integral approximations for LCAO-SCF calculations. *Chem. Phys. Lett.* **1993,** *213* (5), 514-518.
17. Takano, Y.; Houk, K. N., Benchmarking the Conductor-like Polarizable Continuum Model (CPCM) for Aqueous Solvation Free Energies of Neutral and Ionic Organic Molecules. *J. Chem. Theory Comput.* **2005,** *1* (1), 70-77.